



String electrospinning based on the standing wave vibration

Xiaoqing Chen¹ , Youchen Zhang^{1,2,*} , Jiahao Liang³ , Haoyi Li^{1,2} , Mingjun Chen¹ , Lisheng Cheng¹ , Xuetao He¹ , and Weimin Yang^{1,2}

¹ College of Mechanical and Electrical Engineering, Beijing University of Chemical Technology, Beijing 100029, China

² State Key Laboratory of Organic-Inorganic Composites, Beijing 100029, China

³ State Key Laboratory of Heavy Oil Processing, State Key Laboratory of Petroleum Pollution Control, China University of Petroleum-Beijing, Beijing 102249, China

Received: 2 November 2020

Accepted: 27 January 2021

Published online:
16 February 2021

© The Author(s), under exclusive licence to Springer Science+Business Media, LLC part of Springer Nature 2021

ABSTRACT

Preparation of high-quality nanofibers with low applied voltage remains a challenge for needleless electrospinning. In this work, we developed a novel electrospinning technique based on the standing wave vibration of a string. The effects of the process parameters and string parameters on nanofiber diameter and productivity were investigated. The results indicated that standing wave electrospinning is competitive in terms of fiber diameter and productivity when compared with single conventional needle electrospinning. Moreover, the threshold voltage of standing wave electrospinning (18 kV) was approximately 30% lower than most of the current needleless electrospinning techniques (30 kV). The finest nanofiber with a diameter of 173 ± 48 nm was prepared at an applied voltage of 28 kV, a spinning distance of 10 cm, and a standing wave number of 3. The fiber diameter and productivity were significantly influenced by the string diameter and shape instead of the electrical conductivity of the string. The results demonstrated the considerable potential of standing wave electrospinning for fine nanofiber preparation under a low applied voltage.

Introduction

Electrospinning is an efficient and versatile way for nanofiber preparation. It can precisely control nanofiber morphology, diameter, and properties (e.g., specific surface area, nanosize diameter, porosity, weight, and ease of functionalization) by adjusting

the spinning parameters [1, 2]. Various functional nanofibers have been prepared by electrospinning and successfully used for filtration [3], protective cloth [4], biomedicine and biotechnology [5, 6], energy storage [7], and sensors [8, 9]. Electrospinning techniques include single-needle, multiple needles, and needleless (free surface) electrospinning.

Handling Editor: Gregory Rutledge.

Address correspondence to E-mail: zhangyc@mail.buct.edu.cn

Needleless electrospinning has recently gained considerable interest because it addresses the problem of low productivity and needle clogging in needle-type electrospinning. Needleless electrospinning can produce numerous jets forming from the open free surface under a certain electric field strength in the absence of needles. It avoids the blockage of needles and significantly improves spinning efficiency and fiber throughput, thus providing a feasible way for the industrialization of electrospinning [10, 11].

Spinneret geometry (including shape and size) is an essential parameter for needleless electrospinning. It can affect the electric field distribution, which in turn affect the diameter, morphology, and throughput of the prepared nanofibers [12, 13]. Jirsak et al. [14] realized nanofiber preparation through a spinneret with the shape of a cylinder rotating roller. The nanofiber productivity was significantly improved compared with that of conventional needle electrospinning. To date, various geometries of electrospinning spinnerets have been reported, including cone spinnerets [15, 16], ball-shaped spinnerets [17, 18], disk-like spinnerets [13, 19–22], ring-shaped spinnerets [23–25], stepped pyramid spinneret [22, 26], and wire electrodes [27]. These spinnerets have improved the quality and productivity of nanofibers. However, the applied voltages are generally up to 30 kV. High voltage may cause an air breakdown and even an explosion, and other potential safety problems.

Low applied voltage for safe consideration and high-quality nanofiber preparation is important for future needleless electrospinning development. Although free surface electrospinning methods can significantly improve the nanofiber quality and productivity, they cannot effectively control the liquid trigger positions that produce the jets. Most of them require a relatively high applied voltage during the spinning process. Moreover, needle-free electrospinning occurs in the free liquid surface and is a self-organizing process. Accordingly, the number and distribution of jets are difficult to control [10, 28]. Wire-like spinneret was firstly reported by Elmarco company [29], which can prepare nanofibers under a relatively low applied voltage. Subsequently, Forward et al. [30, 31] developed a kind of wire electrodes that could produce jets at an applied voltage of 25 kV. However, the nanofiber diameter was approximately 700 nm. In our previous study, we found that the nanofiber diameter decreased to

143 nm with an assisted mechanical force at the same applied voltage (25 kV) [32]. The plucked string provides kinetic energy for the droplet, which contributes to the excitation of the jet and the refinement of the fiber. The standing wave string is more regular in comparison with the plucked string, which is favorable for the preparation of uniform nanofibers. However, to date, the use of the standing wave string for electrospinning has not been reported. The potential for electrospinning and electric field distribution is still unknown.

In this work, a new electrospinning device based on the string standing wave was proposed. The performance and spinning mechanism were investigated. The spinning process was also optimized, including standing wave number, applied voltage, and collection distance. In addition, we investigated the influences of string parameters (e.g., diameter, conductivity, and shape) on fiber diameter and productivity. Furthermore, simulations of string motion and electric field were performed to reveal the enhancement mechanism. This work demonstrated the considerable potential of the string spinneret, which could achieve high-quality nanofiber preparation with a lower applied voltage.

Experimental

Materials

Polyvinyl alcohol (PVA1799, $M_w = 73900\text{--}82700$; 98–100% hydrolyzed) was supplied by Chenqi Chemical Technology Company (Shanghai, China). The surfactant sodium dodecyl sulfate (SDS) was purchased from Xilong Chemical Technology Corporation (Guangdong, China). PVA powders (66.67 g) were swelled in deionized water for 30 min at 30 °C prior to dissolution. The swelled PVA was dissolved in 600 mL deionized water and stirred (200 r min^{-1}) for 3 h at a temperature of 90 °C. The string was purchased from Alice Guitar of Guangzhou Romance Musical Instruments Co., Ltd. (Guangdong, China).

Standing wave electrospinning setup

The standing wave electrospinning apparatus is presented in Fig. 1a. It consists of six components: frequency regulator self-created, oscillator, string,

solution reservoir, high-voltage DC supply, and receiver plate. High-voltage static electricity is connected to one end of the string (Tianjin Dongwen Company, the upper limit for 80 kV), and the receiver plate is grounded. The string is set across the top of the solution reservoir. The solution reservoir is made of polytetrafluoroethylene (PTFE). A receiver plate made of bronze with a thickness of 1 mm is set vertically above the solution reservoir. The number of standing waves is tuned by adjusting the output power of the frequency regulator. When the string moves into the state of standing wave motion and immersed in a viscous solution, a thin ring shaped of solution was formed around the string. Next, the fluid diffused on the surface of the string is broken to form liquid droplets. The droplets overcome surface tension forming Taylor cones and consequently initiate jets (shown in Fig. 1b). The spinning parameters are summarized in Table 1. The performance of standing wave electrospinning was compared to the single-needle electrospinning. The single-needle electrospinning setup used was designed and made according to a typically reported device [33]. The applied voltage and collection distance for single-needle spinning were 28 kV and 10 cm. The experiments were carried out at a relative humidity of $20 \pm 5\%$ and room temperature of $16 \pm 2^\circ\text{C}$.

Characterization and measurements

Scanning electron microscopy (SEM, JSM7610F, Hitachi, Japan) was used for the morphology and diameter characterization of the electrospun

Table 1 Standing wave spinning conditions

Parameters	Values
PVA solution concentration	10 wt%
PVA solution density	1026 kg m^{-3}
PVA solution viscosity	2.04 Pa S
PVA solution conductivity	$865 \mu\text{s cm}^{-1}$
Applied voltage	20–32 kV
Spinning distance	8–14 cm
Standing wave number	2–5
String diameter	0.6–1.35 mm
l (string length)	600 mm
A (standing wave amplitude)	8 mm
Room temperature	$16 \pm 2^\circ\text{C}$
Relative humidity	$20 \pm 5\%$

nanofibers. The average diameters of the nanofibers from the SEM images were calculated by Image-Pro + 6.0 software. The electrospinning processing photograph was taken with a digital camera (Canon 600D, Canon, China). The PVA solution viscosity was determined using a digital viscometer (NDJ-5S, nerun Intelligent, China). The solution conductivity was determined using a resistivity tester (SZT-C, Suzhou Jingge, China). The string stiffness was measured with Wdw-100 kN electronic universal testing machine (INSTRON 5982, INSTRON, American). The production of nanofibers was calculated by continuously electrospinning for 20 min and then weighting the collected nanofibers with an electronic balance (B3M220, Shanghai Zhuojing, China) [13, 34].

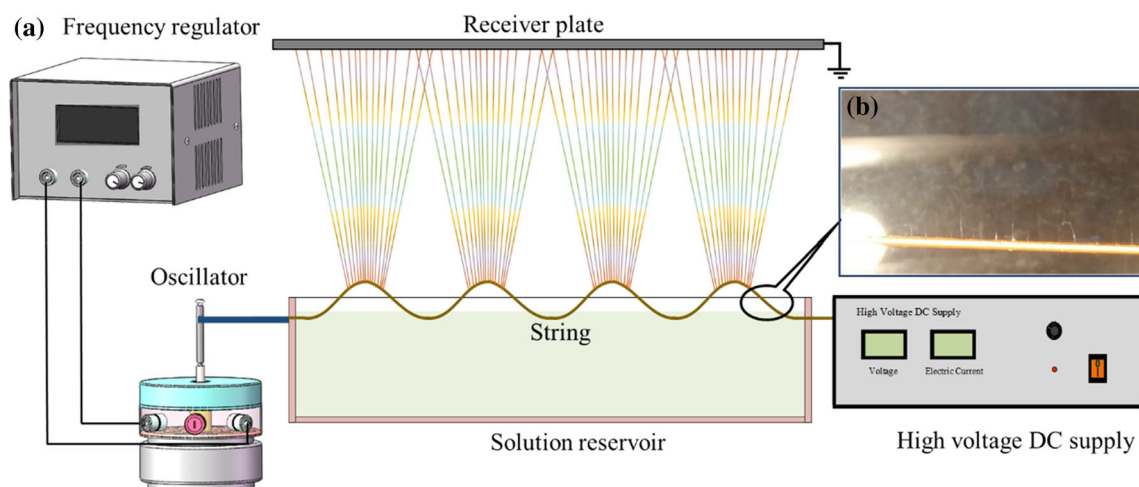


Figure 1 a Schematic diagram of standing waves electrospinning apparatus, b the image of jets forming in the electrospinning process.

Numerical simulations

Simulation of the string standing wave

String vibration is essential for standing wave electrospinning because it leads to the periodic motion and deformation of spinning droplets directly. The string vibration also influences the electric field distribution, which consequently affect the fiber diameter and productivity. Fully understanding the string vibration could help to analyze the distribution of the electric field and the spinning mechanism. The equations of standing wave motion are as follows:

$$\text{Incident wave : } y_1 = A \sin 2\pi \left(ft - \frac{x}{\lambda} \right) = A \sin(\omega t - kx) \quad (1)$$

$$\text{Reflected wave : } y_2 = A \sin 2\pi \left(ft + \frac{x}{\lambda} \right) \\ = A \sin(\omega t + kx) \quad (2)$$

where x is the coordinate of particle position; t is the vibration time; f is the input frequency; A is the amplitude; $\omega = 2\pi f$ is the circular frequency; $k = 2\pi/\lambda$ is the wave vector; λ is the wavelength.

Combination of the incident wave and the reflected wave, the vibration equation and edge condition are as described:

$$\begin{cases} y = y_1 + y_2 = 2A \sin\left(\frac{\pi n}{l}x\right) \cos(2\pi ft) \\ y(l, t) = 0 \end{cases} \quad (3)$$

The simulation of the string standing wave motion was calculated using MATLAB R2016B software (Fig. 3a, b).

Simulation of electric fields

The electric field profile of the string standing wave in the spinning zone was computed by Ansoft Maxwell 3D (ANSYS Corporation) based on the finite element method. Solidworks software was used for the 3D structure model building according to the real size. Then the model was imported into Ansoft Maxwell. The calculating model was built according to the equation $E = -\Delta V$ (where V is the electric potential and E is the strength of the electric field). The default settings of the software were adopted for the mesh generation and solving processes.

Results and discussion

Performance of standing wave electrospinning

This study demonstrated that standing wave electrospinning is a feasible method for fabricating nanofibers. The nanofiber quality and productivity were compared with single-needle electrospinning in this study. The SEM images (Fig. 2a, b) show that the nanofiber quality of standing wave electrospinning was superior to single-needle electrospinning, as reflected in the nanofiber standard deviation and diameter. The average diameter of the nanofibers prepared by standing wave electrospinning was 173 ± 48 nm, finer than those for single-needle (262 ± 89 nm) (Fig. 2c). The finer fibers of standing wave electrospinning might have contributed to the extra inertial force of the string vibration, allowing for the sufficient stretch of jets. In addition, the productivity of standing wave electrospinning achieved 1.15 g h^{-1} (corresponding to the unitary length productivity of $1.92 \text{ g h}^{-1} \text{ m}^{-1}$), which was 22-fold higher than that of single-needle electrospinning (0.05 g h^{-1}). The productivity was also comparable to other wire-like spinnerets [31]. The higher nanofiber quality and productivity of standing wave electrospinning can be ascribed to the mechanical vibration, and more uniform jets were produced during the spinning [12]. In addition, the threshold voltage of standing wave electrospinning was 18 kV, which is lower than that in most previous studies, as shown in Table 2. A low applied voltage could improve operational safety. These results demonstrate the potential application of standing wave electrospinning in the spinning field.

Spinning mechanism and electric field distribution

Simulations of the string motion and electric field were performed to reveal the spinning mechanism of standing wave electrospinning. In the spinning process, some droplets were formed on the surface of the string under the string standing wave vibration. These droplets vibrated with the string-gaining inertia force and formed a Taylor-like cone and finally emitted jets under electric field condition. As the jets traveled through the spinning zone, water

Figure 2 SEM images of nanofiber prepared by **a** single-needle electrospinning and **b** standing wave electrospinning. **c** The diameter and productivity of nanofiber prepared from two electrospinning methods. Processing parameters are as follows: applied voltage of 28 kV, collection distance of 10 cm, standing wave number of 3 and solution concentration of 10 wt%.

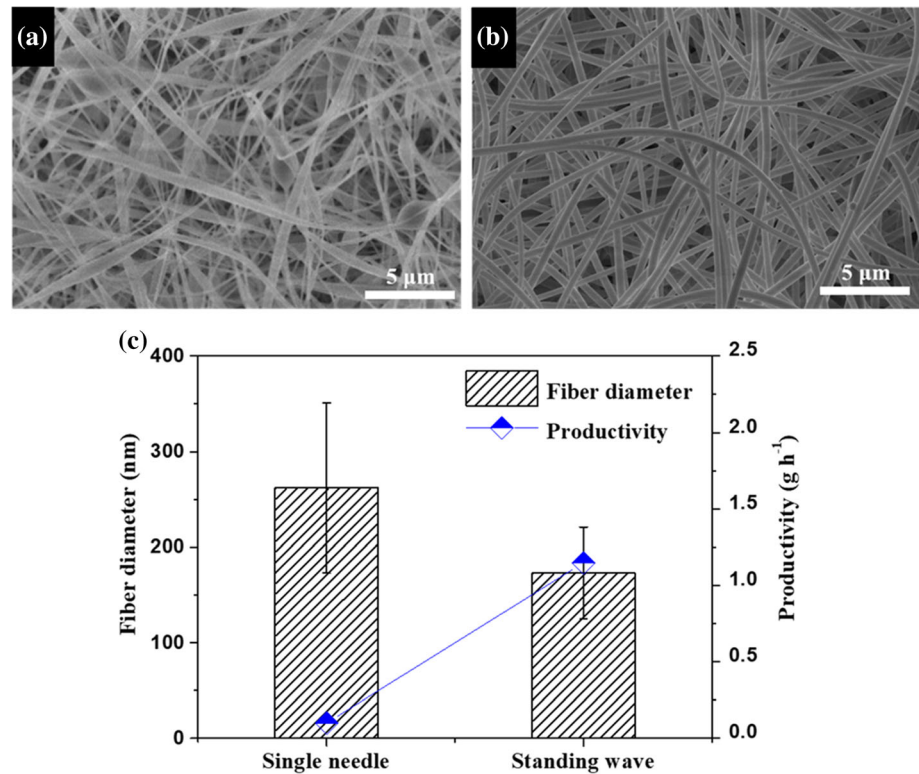


Table 2 Comparison of spinning voltage and electric field intensity between standing wave electrospinning and other electrospinning methods

Spinnerets	Polymer	Voltage (distance)	Average electric field intensity	References
Conical wire coil	PVA	45 kV (15 cm)	3.0 kV cm ⁻¹	[35]
Magnet auxiliary	PEO	32 kV (10 cm)	3.2 kV cm ⁻¹	[36]
Sprocket wheel disk	PVA	50 kV (13 cm)	3.85 kV cm ⁻¹	[37]
Curved convex slot	PVA	55 kV (20 cm)	2.75 kV cm ⁻¹	[34]
Double rings slit	PAN	55 kV (15 cm)	3.67 kV cm ⁻¹	[38]
Metal dish	PAN	50 kV (15 cm)	3.33 kV cm ⁻¹	[39]
Plucked string	PVA	15 kV (7 cm)	2.14 kV cm ⁻¹	[32]
Standing wave string	PVA	20 kV (10 cm)	2.0 kV cm ⁻¹	This study

evaporated and dry solid PVA fibers were deposited on the receiver plate.

The viscous force, gravity, and electric field force are conducive to the liquid layer formation and jets stretching. The force situation of droplets at any given time was associated with string motion (shown in Fig. S1). A few of the droplets were formed on the wave valley of string and got an upward acceleration when the viscous force and electric field force exceeded surface tension and gravity. The droplets were accelerating upward until its velocity was equal to that of string. During this stage, Taylor-like cones and jets were formed. The jets were further stretched at wave crest under the action of strong electric field, reverse viscous force, and gravity. The jets were

further stretched in the spinning zone mainly through electric field force and gravity. Thus, the standing wave electrospinning could achieve higher quality preparation of nanofibers. Compared with a plucked string, the standing wave string had a wide range of adjustable wavenumbers, allowing the formation of more jets to improve productivity. Thus, standing wave electrospinning was competitive in both fiber quality and productivity.

The theoretical analysis of standing wave spinning with a lower applied voltage was mainly explained by the following two aspects. First, the motion of string vibration is important in this electrospinning method, as mentioned before [32]. From the string motion (as shown in Fig. 3a, b), we can observe that

the string is immersed in the spinning liquid and withdraws from the liquid surface periodically. When the string is immersed in the viscous solution, a thin fluid layer forms around it on withdrawal. It is determined by the interaction of viscosity, inertial force, and gravity for the solution retention on the string [10]. At a specific point on the string, when the string moves to a certain height, the thin liquid layer attached to the string is stretched with the assistance of the electric driving force. Next, several Taylor cones are formed spontaneously if the electric field strength is sufficiently large. This is consistent with the basic explanation of Lucas [28] and Miloh [40] that polymeric jets are ejected from a conductive liquid layer at the moment when the electric field strength surpasses a critical value. The string withdraws rapidly after reaching the wave peak in a short time. In this process, the jet with a Taylor cone shape is stretched by an upward electric field force and a downward viscous force and gravity on the liquid

layer, which contributes to jet stretching and refining. Because the string is always in the motion state of a certain frequency, it is speculated that the thin liquid layer is attached to the dynamically unstable string to overcome the surface tension and viscosity resistance. Consequently, it produces protrusions on the string surface, thus promoting the Taylor cone formation and jet excitation and reducing the threshold voltage required for spinning compared with the previously reported wire spinning.

Second, the electric field is significant in the spinning process and closely related to the vibration of the string. When the string moves beyond the liquid surface, the collection distance decreases and the electric field strength increases gradually. Figure 3c, d show the electric field strength from the wave crest is higher than that from the wave node and valley from the same horizontal line. In this process, the Taylor cone easily forms on the string surface and then initiates the jets. The periodic motion of the

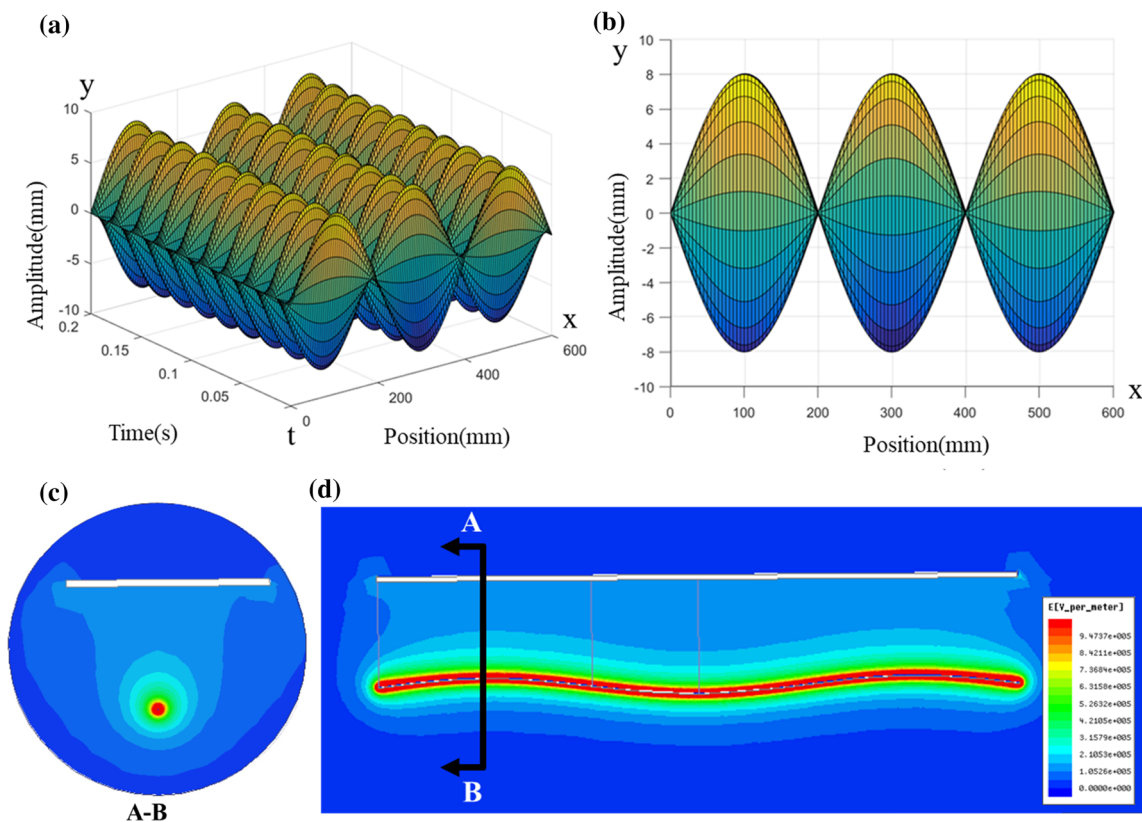


Figure 3 MATLAB simulation of string motion with three standing waves: **a** track of string motion within 0.2 S, **b** the amplitude of different positions on the string; The electric field simulation: **c** cross section (A–B) of electric field distribution at wave crest, **d** the principle section of electric field intensity

distribution in the spinning area with three standing waves. The black arrow was section cut line marked as A–B. The simulation parameter are as follows: input voltage of 28 kV for string and 0 kV for the receiver plate, input frequency of 45 Hz, amplitude of 8 mm and wave length of 450 mm.

string also induces a periodic change in the strength of electric field in the spinning area with the collection distance change. It is assumed that the variation in the electric field also facilitates the emergence of surface protrusions from the liquid layer, thus facilitating the Taylor cone forming and the excitation of the jets, which might be a reason for the lower threshold voltage in the spinning process.

Effects of process parameters on fiber diameter and productivity

Applied voltage

The applied voltage determines the intensity distribution of the electric field and, consequently, the driving force of the jets, which significantly affect the nanofiber diameter and productivity. No jets were found unless the applied voltage exceeded 18 kV. The applied voltage range (20–32 kV) was used to investigate their effects on fiber diameter and productivity. The nanofiber diameter decreased with an increase in the applied voltage, as observed in previous studies [23]. The nanofibers average diameter decreased from 443 ± 75 to 144 ± 39 nm as the voltage increased from 20 to 32 kV (Fig. 4a–d). The stronger intensity of electric field in the spinning zone with a higher voltage leads to higher driving forces and more sufficient stretching for jets in the spinning area, hence refining the nanofiber and reducing the diameter of the nanofibers. In addition, it was assumed that the kinetic energy of droplets provided by the string during periodic motion is also conducive to overcoming the surface tension of the droplet. The productivity of the nanofiber increased significantly with increasing spinning voltage from 20 to 32 kV (Fig. 4e). This was ascribed to the fact that more jets could be induced with a larger electric field intensity under the higher spinning voltage. The optimal applied voltage was determined to be 28 kV, taking into account fiber diameter and productivity.

Collection distance

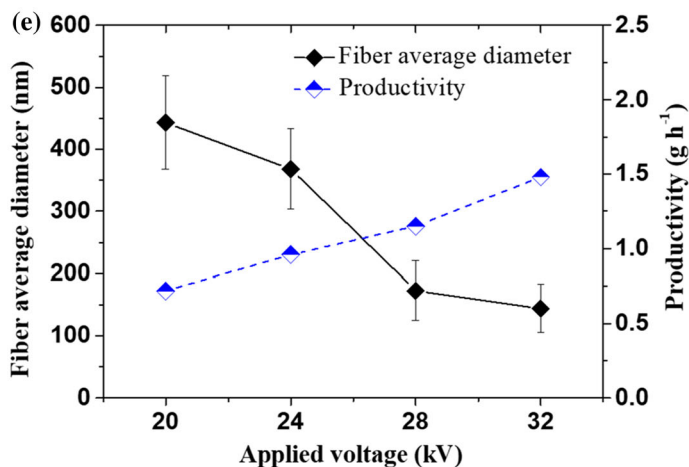
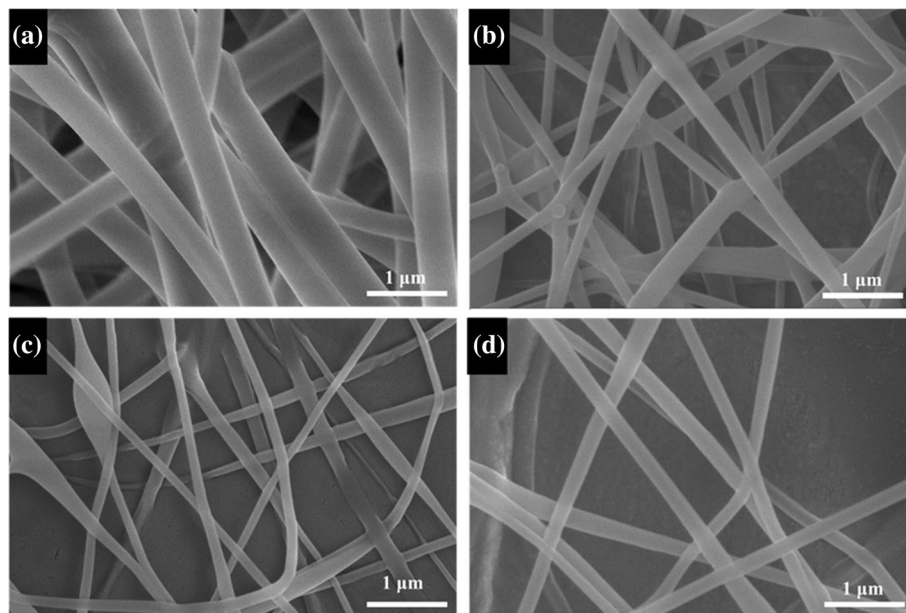
The collection distance is essential for electrospinning. The morphology, diameter, and productivity of the nanofibers prepared at different collection distances are shown in Fig. 5. The fiber diameter displayed a tendency of decreasing first and then increasing, which is agreed with the result of Wei

et al. [24]. The results suggested that the quality of fiber could decrease whether the collection distance was too small or too large. An extremely small collection distance would cause insufficiency of solvent volatilization forming clusters, while an excessively large collection distance would lead to a decrease in the electric field as a result of insufficient stretch force for jets. As shown in Fig. 5a, the nanofibers prepared at a collection distance of 8 cm were observed with some bead formation. The fiber diameter increased from 173 ± 48 to 357 ± 71 nm with the collection distance increasing from 10 to 14 cm. The fiber productivity decreased with an increase in the collection distance (Fig. 5e), which also caused a decrease in the intensity of electric field limiting the formation of jets. Thus, the optimal collection distance was determined to be 10 cm. The nanofiber diameter and productivity were 173 ± 48 nm and 1.15 g h^{-1} , respectively.

Number of standing waves

Based on the energy conservation law, the string wavenumber changes the string amplitude, which, in turn, affects the electric field distribution and consequently influences the nanofiber quality. The nanofiber morphology, diameter, and productivity under different standing wave numbers are shown in Fig. 6. The nanofibers at wavenumber of 2 were uneven and had a wide diameter distribution. The uneven fiber distribution may be attributed to an excessively large string amplitude. A large string amplitude would cause a non-uniform intensity distributing of the electric field, particularly for the position of the wave crest and wave valley. Compared with the nanofibers at wavenumber of 2, the nanofibers at the wavenumber of 3 exhibited a narrower diameter distribution and a smaller averaging diameter. The increased string wavenumber could have caused a decrease in string amplitude, which led to a decrease in the strength of electric field, decreasing the stretching strength. When the standing wave number increased from 3 to 5, the nanofiber diameter increased from 173 ± 48 to 225 ± 28 nm (Fig. 6e). Nanofiber productivity exhibited a positive correlation with the standing wave number. The string with a higher wavenumber had more contact surfaces with the spinning solution, which could increase the number of jets and improve fiber productivity. Considering the homogeneity and productivity, the

Figure 4 SEM images of nanofibers from different applied voltages of **a** 20 kV, **b** 24 kV, **c** 28 kV, **d** 32 kV. **e** The diameter and productivity of nanofiber with different applied voltages. Processing parameters are as follows: collection distance of 10 cm, standing wave number of 3 and solution concentration of 10 wt%.



optimized standing wave number was determined to be 3.

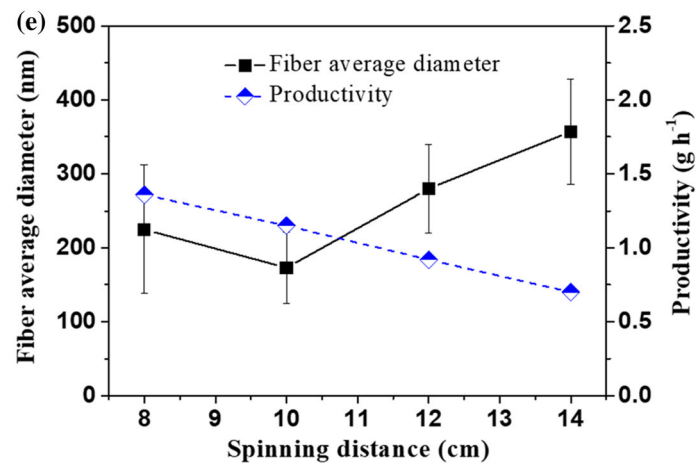
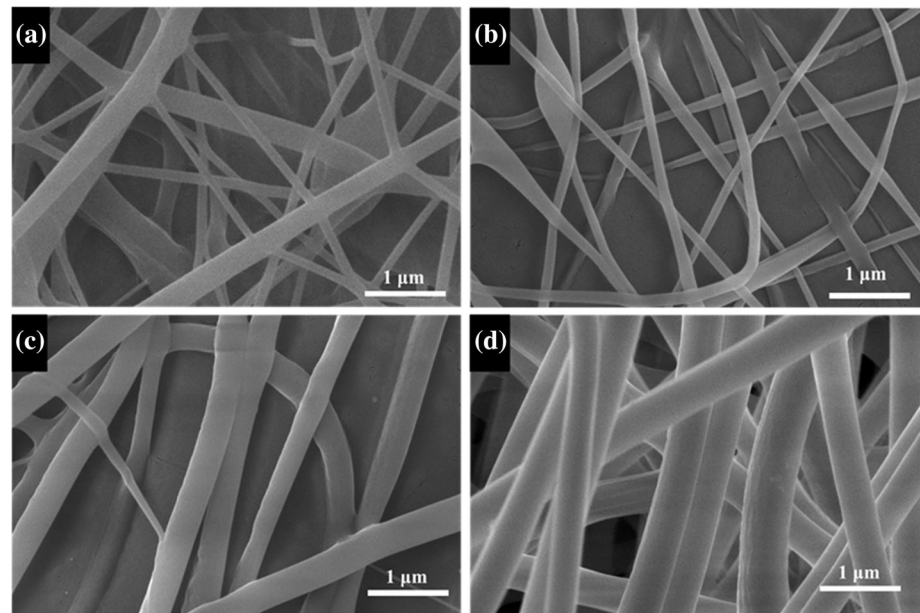
Effects of string parameters on fiber diameter and productivity

Diameter of the string

The diameter, shape, and conductivity of the string were explored to reveal the impacts of string parameters on nanofiber diameter and productivity. Various copper strings with diameters of 0.6, 1.0, and 1.35 mm were used to investigate their effects on nanofiber diameter and productivity. All experiments were performed at a voltage of 28 kV, collection distance of 10 cm, and standing wave number of 3. The nanofiber diameter increased from 153 ± 56 to

245 ± 34 nm as the string diameter increased from 0.6 to 1.35 mm (shown in Fig. 7). The nanofiber diameter was distributed more uniformly with a larger diameter of the string. According to the electric field simulation, the string with a smaller radius had a higher electric field intensity. As shown in Fig. 7e, the intensity of the electric field around the string wave crest, node, and valley with a diameter of 0.6 mm is higher than that with a diameter of 1.0 mm, which made a sufficient stretch of the jets. Thus, an increasing tendency in the fiber diameter was observed with an increase in the string diameter. The nanofiber productivity also increased from 0.89 to 1.54 g h^{-1} (Fig. 7d). This result is ascribed to the larger surface area of the thick string that can provide more jet distribution sites. Simultaneously, the larger diameter string carried more solutions that could also

Figure 5 SEM images of nanofibers from different collection distances: **a** 8 cm, **b** 10 cm, **c** 12 cm, **d** 14 cm. **e** The diameter and productivity of nanofiber with different collection distances. Processing parameters are as follows: applied voltage of 28 kV, standing wave number of 3 and solution concentration of 10 wt%.



facilitate fiber productivity. This experimental result is also consistent with the conclusion of previous reports [41].

Conductivity of string

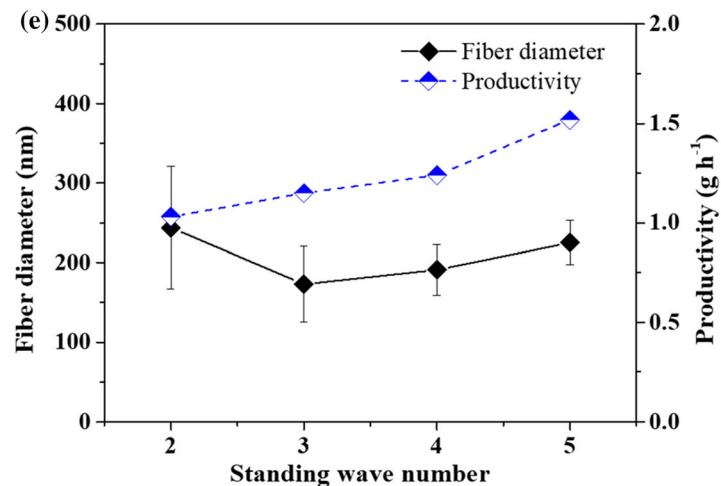
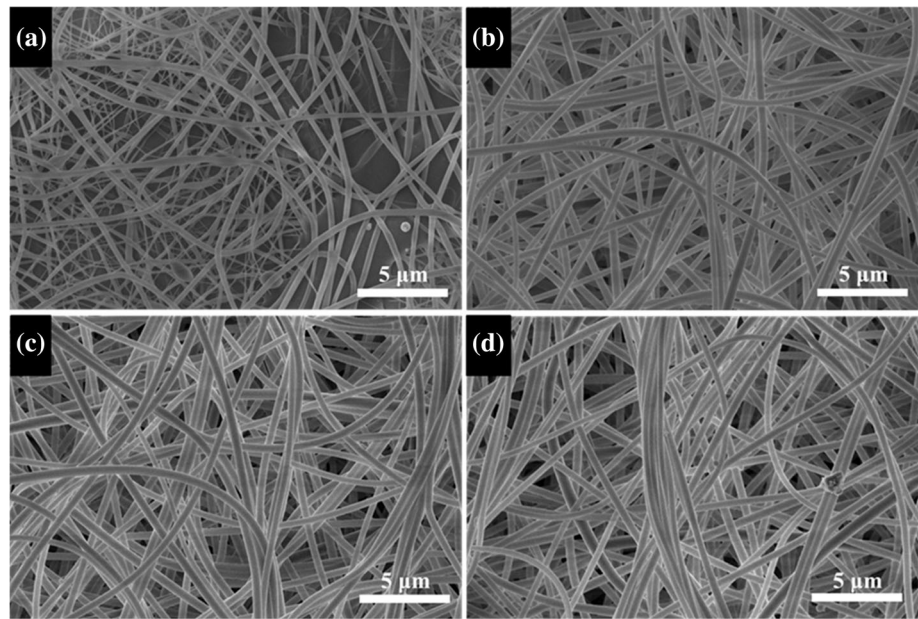
Bronze and steel stainless strings were selected to explore the impact of string conductivity on the diameter and productivity of nanofibers because of their significant difference in conductivity ($5.8 \times 10^7 \text{ S m}^{-1}$ vs. $1.1 \times 10^6 \text{ S m}^{-1}$). As shown in Fig. 8, the nanofiber diameter prepared with steel stainless string was similar with that prepared with a bronze string, although its conductivity was quite different. In addition, productivity was nearly the same. This is attributed to the fact that the voltage along the conductive string was the same, and the

electric fields between the string and receiver plate were nearly identical. Therefore, there is a small difference in the stretching forces of the jets in the electric field. The distribution of electric field intensity with two strings of bronze and stainless steel with different conductivity is shown in Fig. S2. Based on this result, ordinary conductive metal materials with soft characteristics would be suitable if the cost is considered.

The shape of the string

To evaluate the impacts of the string shape on the prepared nanofibers, two strings with smooth and protruding surfaces were selected. The string was self-made from steel stainless with a diameter of 1.0 mm. The protrusion was designed as a small cone

Figure 6 SEM images of nanofibers from different standing wave numbers: **a** two, **b** three, **c** four, **d** five. **e** The diameters and productivity of nanofiber with different standing wave numbers. Processing parameters are as follows: collection distance of 10 cm, applied voltage of 28 kV and solution concentration of 10 wt%.



with a height of 0.5 mm and radius of 0.6 mm, distributed linearly on the string surface. The effects of two different string shapes on nanofiber morphology, diameter, and productivity are presented in Fig. 9. The diameter distribution of the nanofibers with a smooth surface was relatively uniform, with an average diameter of 173 ± 48 nm and productivity of 1.15 g h^{-1} . The average diameter of the nanofiber prepared by the string with protrusion was 205 ± 121 nm, and the productivity was 2.32 g h^{-1} . The average fiber diameter prepared by the string with protrusion was larger than that of the smooth surface but did not vary considerably. However, the standard deviation and productivity were much higher than that of the smooth surface. This may be attributed to the uneven size distribution of the

solution droplets dipped on the string with protrusion, and the natural point effect of electric field intensity distribution on the protrusion instead of the smooth string (Fig. 9c–d). In terms of fiber productivity, this is mainly due to the fact that string with protrusion significantly increases the surface area of the string. Thus, it could carry more solution droplets and provide more jet distribution sites on the string surface.

Conclusion

It was demonstrated that string electrospinning based on standing waves was a feasible method to prepare nanofibers at a low applied voltage. The

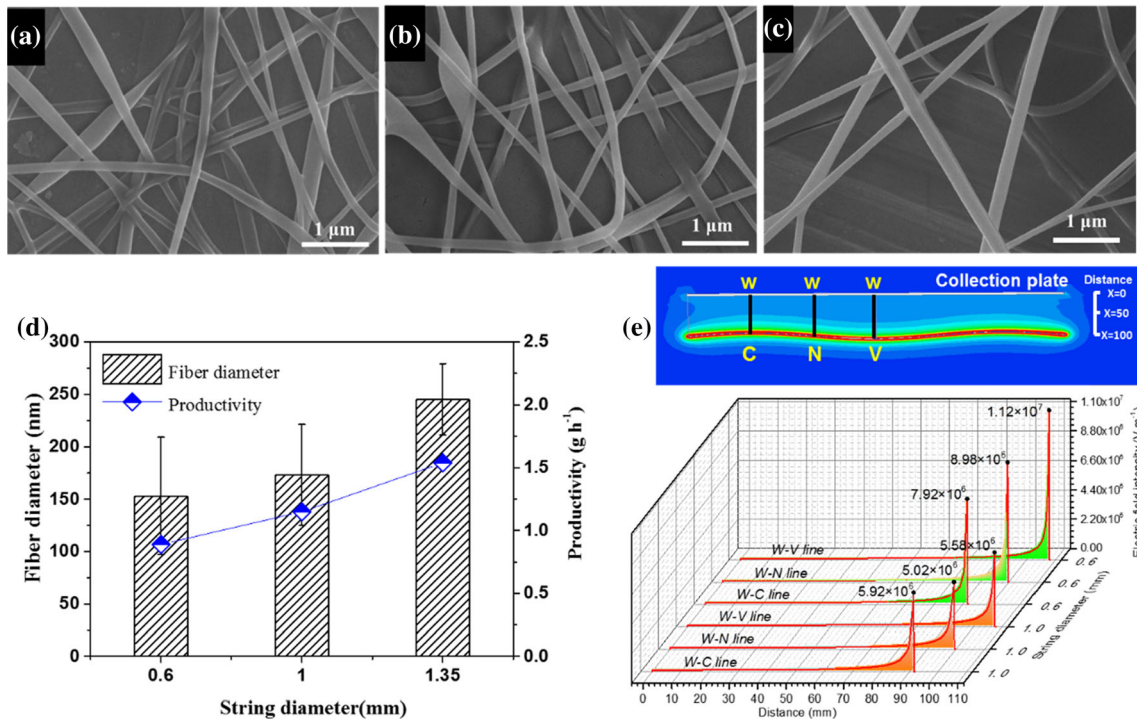


Figure 7 SEM images of nanofibers from different string diameters: **a** 0.6 mm, **b** 1.0 mm and, **c** 1.35 mm. **d** Diameters and productivity of nanofiber with different string diameters. **e** The electric field intensity distribution with string diameters of 0.6 and

1.0 mm. The lines W–C, W–N and W–V are respectively linked from collection plate to the wave crest, wave node and wave valley of string.

Figure 8 **a** SEM image of nanofibers from bronze ($5.8 \times 10^7 \text{ S m}^{-1}$) and **b** SEM image of nanofiber from stainless steel ($1.1 \times 10^6 \text{ S m}^{-1}$). **c** The diameters and productivity of nanofibers from string with different conductivity.

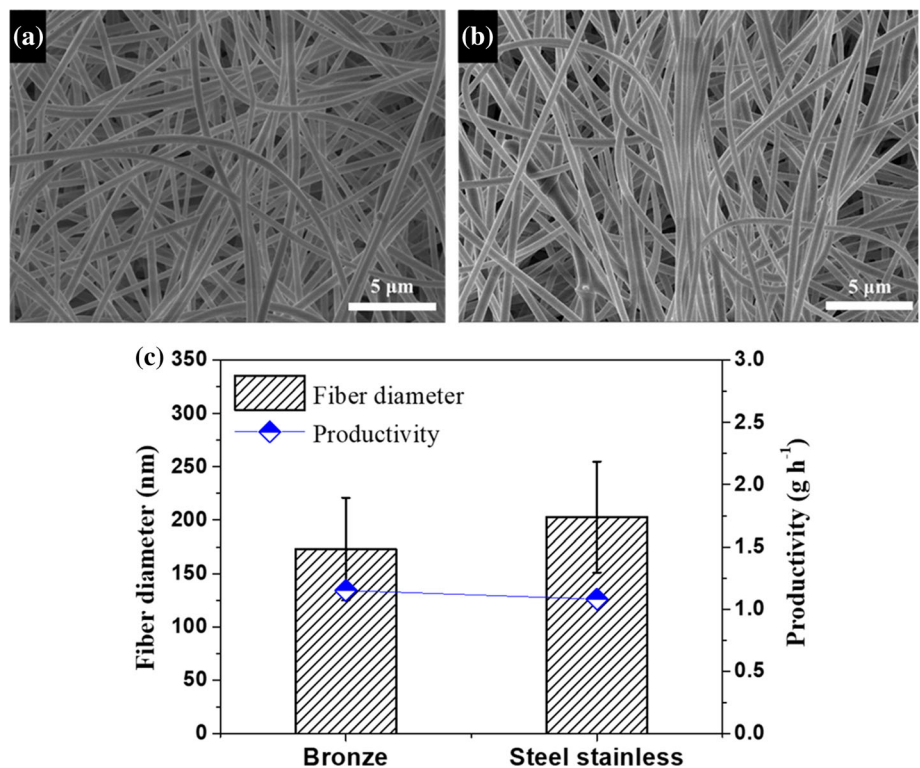
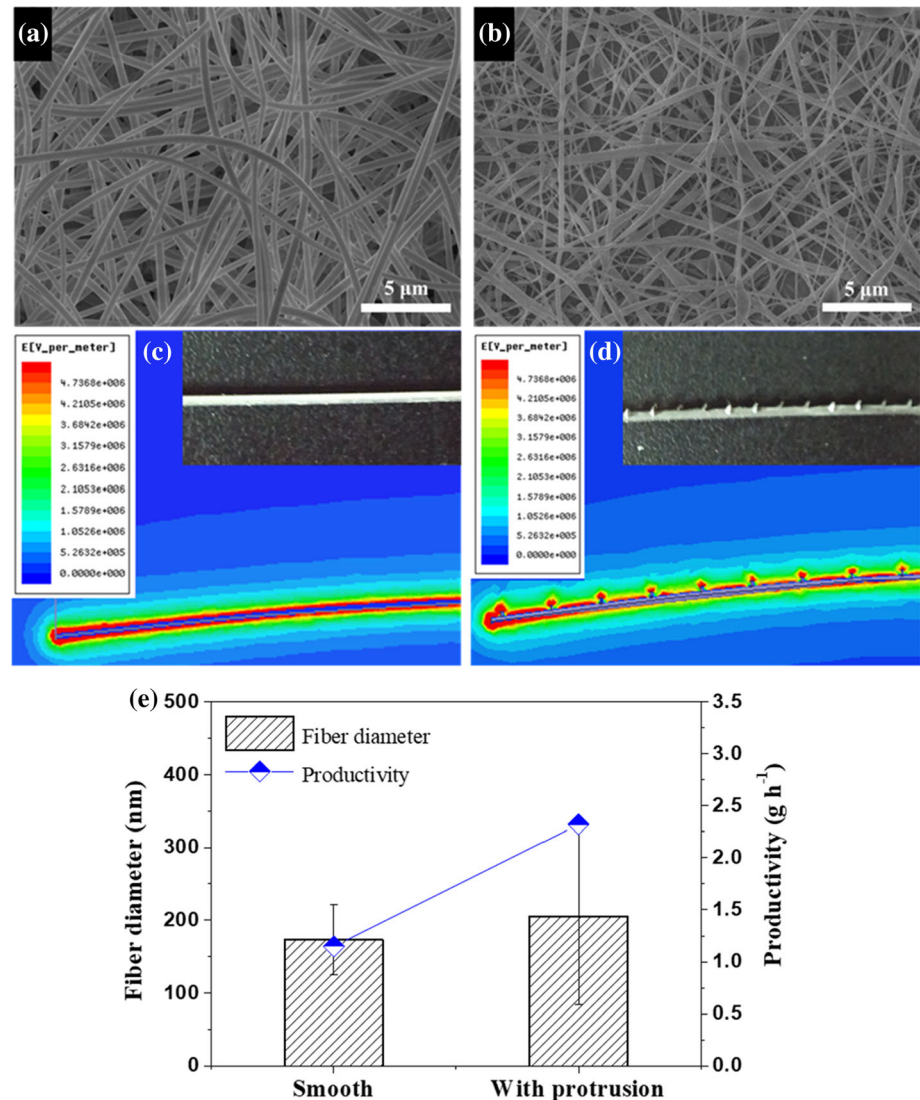


Figure 9 **a** SEM images of the nanofibers with smooth surface of string and **b** SEM images of the nanofibers with protrusion of string. **c** The diameter and productivity of nanofiber from two types of string.



threshold voltage of string electrospinning was 18 kV, which is lower than that reported in most of previous studies (≥ 30 kV). Both nanofiber quality and productivity by standing wave electrospinning were superior to single-needle electrospinning. The finest nanofiber with a diameter of 173 ± 48 nm was obtained at a spinning distance of 10 cm, applied voltage of 28 kV, and standing wave number of 3. Under these conditions, the nanofiber productivity achieved 1.15 g h^{-1} , being 22-fold higher than single-needle electrospinning. Moreover, the productivity could be improved further by installing multiple strings; thus, standing wave electrospinning has a promising application in spinning. The analysis of string parameters demonstrated that the string

diameter and shape had significant effects on nanofiber diameter and productivity, whereas no notable effects were found in string conductivity. This work demonstrated the considerable potential of standing wave electrospinning in the field of spinning, which simultaneously achieved high-quality nanofiber preparation and low applied voltage.

Acknowledgements

This work was supported by the National Key Research and Development Program (grant no. 2016YFB0302002).

Compliance with ethical standards

Conflict of interest It was declared that authors have no competing of any interests.

Supplementary information: The online version contains supplementary material available at <https://doi.org/10.1007/s10853-021-05845-x>.

References

- [1] Yu M, Dong R-H, Yan X, Yu G-F, You M-H, Ning X, Long Y-Z (2017) Recent advances in needleless electrospinning of ultrathin fibers: from academia to industrial production. *Macromol Mater Eng* 302:1700002. <https://doi.org/10.1002/mame.201700002>
- [2] Yang D, Li L, Chen B, Shi S, Nie J, Ma G (2019) Functionalized chitosan electrospun nanofiber membranes for heavy-metal removal. *Polymer* 163:74–85
- [3] Qin XH, Wang SY (2006) Filtration properties of electrospinning nanofibers. *Appl Polym Sci* 02(2):1285–1290
- [4] Dhineshbabu NR, Karunakaran G, Suriyaprabha R, Manivasakan P, Rajendran V (2014) Electrospun MgO/Nylon 6 hybrid nanofibers for protective clothing. *Nano-Micro Lett* 6(1):46–54
- [5] Venugopal J, Ramakrishna S (2005) Applications of polymer nanofibers in biomedicine and biotechnology. *Appl Biochem Biotechnol* 125(3):147–157
- [6] Ghosal K, Agatemor C, Špitálský Z, Thomas S, Kny E (2019) Electrospinning tissue engineering and wound dressing scaffolds from polymer-titanium dioxide nanocomposites. *Chem Eng J* 358:1262–1278
- [7] Li L, Peng S, Lee JKY, Ji D, Srinivasan M, Ramakrishna S (2017) Electrospun hollow nanofibers for advanced secondary batteries. *Nano Energy* 39:111–139
- [8] Ding B, Wang M, Yu J, Sun G (2009) Gas sensors based on electrospun nanofibers. *Sensors* 9(3):1609–1624
- [9] Gao J, Li B, Huang X, Wang L, Lin L, Wang H, Xue H (2019) Electrically conductive and fluorine free superhydrophobic strain sensors based on SiO₂/graphene-decorated electrospun nanofibers for human motion monitoring. *Chem Eng J* 373:298–306
- [10] Akampumuza O, Gao H, Zhang H, Wu D, Qin XH (2018) Raising nanofiber output: the progress, mechanisms, challenges, and reasons for the pursuit. *Macromol Mater Eng* 303(1):1700269. <https://doi.org/10.1002/mame.201700269>
- [11] SalehHudin H, Sofia M, Edzrol N, Mahadi W, Nor L (2018) Multiple-jet electrospinning methods for nanofiber processing: a review. *Mater Manuf Processes* 33(5):479–498
- [12] Niu H, Lin T (2012) Fiber generators in needleless electrospinning. *J Nanomater* 2012:1–13
- [13] Ali U, Niu H, Aslam S, Jabbar A, Rajput AW, Lin T (2017) Needleless electrospinning using sprocket wheel disk spinneret. *J Mater Sci* 52(12):7567–7577. <https://doi.org/10.1007/s10853-017-0989-6>
- [14] Jirsak O, Sanetnik F, Lukas D, Kotek V, Martinova L, Chaloupek J (2009) Method of nanofibres production from a polymer solution using electrostatic spinning and a device for carrying out the method. US Patent.
- [15] Lu B, Wang Y, Liu Y, Duan H, Zhou J, Zhang Z, Wang Y, Li X, Wang W, Lan W (2010) Superhigh-throughput needleless electrospinning using a rotary cone as spinneret. *Small* 6(15):1612–1616
- [16] Wang X, Xu W (2011) Effect of experimental parameters on needleless electrospinning from a conical wire coil. *Appl Polym Sci* 123(6):3703–3709
- [17] Zhang Y, Cheng Z, Han Z, Zhao S, Zhao X, Kang L (2018) Stable multi-jet electrospinning with high throughput using the bead structure nozzle. *RSC Adv* 8(11):6069–6074
- [18] Xiong J, Zhou M, Zhang H, Quan Z, Wang R, Qin X (2018) Sandwich-structured fibrous membranes with low filtration resistance for effective PM_{2.5} capture via one-step needleless electrospinning. *Mater Res Express* 6(3):035027. <https://doi.org/10.1088/2053-1591/aaf760>
- [19] Liu Z, Ang KKJ, He J (2017) Needle-disk electrospinning inspired by natural point discharge. *J Mater Sci* 52(4):1–8. <https://doi.org/10.1007/s10853-016-0472-9>
- [20] Liu Z, Chen R, He J (2016) Active generation of multiple jets for producing nanofibres with high quality and high throughput. *Mater Des* 94:496–501
- [21] Zhang Y, Zhang L, Cheng L, Qin Y, Li Y, Yang W, Li H (2018) Efficient preparation of polymer nanofibers by needle roller electrospinning with low threshold voltage. *Polym Eng Sci* 59(4):745–751
- [22] Jiang GJ, Zhao WM, Qin XH (2014) Composite nanofibers containing microparticles produced via a stepped pyramid-shaped spinneret. *Adv Mater Res* 893:149–152
- [23] Wei L, Qiu Q, Wang R, Qin X (2018) Influence of the processing parameters on needleless electrospinning from double ring slits spinneret using response surface methodology. *Appl Polym Sci* 135(27):46407. <https://doi.org/10.1002/app.46407>
- [24] Wei L, Sun R, Liu C, Xiong J, Qin X (2019) Mass production of nanofibers from needleless electrospinning by a novel annular spinneret. *Mate Des* 179:107885. <https://doi.org/10.1016/j.matdes.2019.107885>
- [25] Jahan I, Wang L, Wang X (2019) Needleless electrospinning from a tube with an embedded wire loop. *Macromol Mater*

- Eng 304(3):1800588. <https://doi.org/10.1002/mame.201800588>
- [26] Jiang G, Zhang S, Qin X (2013) High throughput of quality nanofibers via one stepped pyramid-shaped spinneret. *Mater Lett* 106:56–58
- [27] Hsieh CT, Lou CW, Pan YJ, Huang CL, Chiang KC (2016) Fabrication of poly(vinyl alcohol) nanofibers by wire electrode-incorporated electrospinning. *Fibers Polym* 17(8):1217–1226
- [28] Lukas D, Sarkar A, Pokorny P (2008) Self-organization of jets in electrospinning from free liquid surface: a generalized approach. *J Appl Phys* 103(8):084309. <https://doi.org/10.1063/1.2907967>
- [29] Green TB, King SL, Li L (2011) Fine fiber electrospinning equipment, filter media systems and methods. US 2011/0223330 A1, United States
- [30] Forward KM, Rutledge GC (2012) Free surface electrospinning from a wire electrode. *Chem Eng J* 183:492–503
- [31] Bhattacharyya I, Molaro MC, Braatz RD, Rutledge GC (2016) Free surface electrospinning of aqueous polymer solutions from a wire electrode. *Chem Eng J* 289:203–211
- [32] Chen X, Zhang Y, He X, Li H, Wei B, Yang W (2019) Electrospinning on a plucked string. *J Mater Sci* 54(1):901–910. <https://doi.org/10.1007/s10853-018-2870-7>
- [33] Sun B, Long YZ, Yu F, Li MM, Zhang HD, Li WJ, Xu TX (2012) Self-assembly of a three-dimensional fibrous polymer sponge by electrospinning. *Nanoscale* 4(6):2134–2137
- [34] Yan G, Niu H, Shao H, Zhao X, Zhou H, Lin T (2017) Curved convex slot: an effective needleless electrospinning spinneret. *J Mater Sci* 52(19):11749–11758. <https://doi.org/10.1007/s10853-017-1315-z>
- [35] Xin W, Niu H, Tong L, Wang X (2010) Needleless electrospinning of nanofibers with a conical wire coil. *Polym Eng Sci* 49(8):1582–1586
- [36] Yarin AL, Zussman E (2004) Upward needleless electrospinning of multiple nanofibers. *Polymer* 45(9):2977–2980
- [37] Ali U, Niu H, Aslam S, Jabbar A, Rajput AW, Lin T (2017) Needleless electrospinning using sprocket wheel disk spinneret. *J Mater Sci* 52(12):1–11. <https://doi.org/10.1007/s10853-017-0989-6>
- [38] Wei L, Zhang H, Qin X (2019) Fabricated narrow diameter distribution nanofiber for an air filtration membrane using a double rings slit spinneret. *Text Res J* 89(6):936–947. <https://doi.org/10.1177/0040517518758009>
- [39] Wei L, Yu H, Jia L, Qin X (2018) High-throughput nanofiber produced by needleless electrospinning using a metal dish as the spinneret. *Text Res J* 88(1):80–88
- [40] Miloh T, Spivak B, Yarin A (2009) Needleless electrospinning: Electrically driven instability and multiple jetting from the free surface of a spherical liquid layer. *J Appl Phys* 106(11):114910. <https://doi.org/10.1063/1.3264884>
- [41] Wu X-F, Zhou Z, Zholobko O, Jenniges JJ, Baatz B, Ahmadi M, Chen J (2020) Critical condition of electrohydrodynamic jetting from a polymer-solution droplet on a conductive wire. *J Appl Phys* 127(5):054303. <https://doi.org/10.1063/1.5132313>

Publisher's Note Springer Nature remains neutral with regard to jurisdictional claims in published maps and institutional affiliations.